HHS Public Access

Author manuscript

Kidney Int. Author manuscript; available in PMC 2019 February 01.

Published in final edited form as:

Kidney Int. 2018 February ; 93(2): 403–415. doi:10.1016/j.kint.2017.08.005.

Adenylyl cyclase 5 deficiency reduces renal cyclic AMP and cyst growth in an orthologous mouse model of polycystic kidney disease

Qian Wang[1], **Patricia Cobo-Stark**[1], **Vishal Patel**[1], **Stefan Somlo**[2], **Pyung-Lim Han**[3], and **Peter Igarashi**[1,4]

[1]Department of Internal Medicine, University of Texas Southwestern Medical Center, Dallas, Texas, USA

[2]Departments of Internal Medicine and Genetics, Yale Medical School, New Haven, CT, USA

[3]Department of Brain and Cognitive Sciences, Brain Disease Research Institute, and Department of Chemistry and Nano Science, Ewha Womans University, Seoul, Korea

[4]Department of Medicine, University of Minnesota Medical School, Minneapolis, MN, USA

Abstract

Cyclic AMP promotes cyst growth in polycystic kidney disease (PKD) by stimulating cell proliferation and fluid secretion. Previously, we showed that the primary cilium of renal epithelial cells contains a cAMP regulatory complex comprising adenylyl cyclases 5 and 6 (AC5/6), polycystin-2, A-kinase anchoring protein 150, protein kinase A, and phosphodiesterase 4C. In *Kif3a* mutant cells that lack primary cilia, the formation of this regulatory complex is disrupted and cAMP levels are increased. Inhibition of AC5 reduces cAMP levels in *Kif3a* mutant cells, suggesting that AC5 may mediate the increase in cAMP in PKD. Here, we examined the role of AC5 in an orthologous mouse model of PKD caused by kidney-specific ablation of *Pkd2*. Knockdown of AC5 with siRNA attenuated the increase in cAMP levels in *Pkd2*-deficient renal epithelial cells. Levels of cAMP and AC5 mRNA transcripts were elevated in the kidneys of mice with collecting duct-specific ablation of *Pkd2*. Compared with *Pkd2* single mutant mice, AC5/*Pkd2* double mutant mice had less kidney enlargement, lower cyst index, reduced kidney injury, and improved kidney function. Importantly, cAMP levels and cAMP-dependent signaling were reduced in the kidneys of AC5/*Pkd2* double mutant compared to the kidneys of *Pkd2* single mutant mice. Additionally, we localized endogenous AC5 in the primary cilium of renal epithelial cells and showed that ablation of AC5 reduced ciliary elongation in the kidneys of *Pkd2* mutant mice. Thus, AC5 contributes importantly to increased renal cAMP levels and cyst growth in *Pkd2* mutant mice, and inhibition of AC5 may be beneficial in the treatment of PKD.

Correspondence: Peter Igarashi, Department of Medicine, University of Minnesota Medical School, 420 Delaware St. SE, MMC 194, Minneapolis, MN, 55455, USA. Phone: 1-612-625-3654. Fax: 1-612-626-3055. igarashi@umn.edu.

DISCLOSURE

Dr. Stefan Somlo receives equity and consulting fees from Goldfinch Biopharma.

Keywords

Polycystic kidney disease; adenylyl cyclase; cyclic AMP; polycystin-2; cilia; knockout mice

INTRODUCTION

Autosomal dominant polycystic kidney disease (ADPKD) is the most common renal cystic disorder, affecting approximately 1 in 500 individuals, and represents the fourth leading cause of end-stage kidney disease in adults[1]. ADPKD is caused by mutations in *PKD1* (encoding polycystin-1) or *PKD2* (encoding polycystin-2). Polycystin-1 (PC1) is an integral membrane protein containing 11 transmembrane segments and a large, receptor-like extracellular N-terminal domain. Polycystin-2 (PC2) contains six transmembrane segments and functions as a Ca^{2+}-permeable transient receptor potential (TRP) channel. Although PC2 is mainly located in the endoplasmic reticulum, PC1/PC2 heterodimers are found in primary cilia in renal tubular epithelial cells[2, 3]. Primary cilia are sensory organelles that are found on the surface of most cells. Primary cilia are composed of a microtubule-based axoneme that emerges from the basal body and is surrounded by the ciliary membrane. Most renal epithelial cells contain a solitary primary cilium that projects from the apical surface into the tubular lumen. Renal cilia are thought to function as mechanosensors that respond to fluid flow and regulate intracellular Ca^{2+} [4], although this latter function has recently been challenged[5]. Renal cilia also express receptors for ligands such as somatostatin and vasopressin and bind urinary exosomes[6–8]. PKD is the prototype of a ciliopathy, a group of pleiotropic genetic disorders that are characterized by abnormalities in the function or structure of the primary cilium and/or basal body. In support of this notion, we have previously shown that KIF3A (Kinesin Family Member 3A), a motor protein that mediates intraflagellar transport, is required for renal ciliogenesis[9]. Kidney-specific ablation of *Kif3a* results in the loss of renal cilia and is sufficient to produce kidney cysts. In addition, a cilia-dependent cyst-activating mechanism has recently been uncovered[10].

The second messenger adenosine 3′,5′-cyclic monophosphate (cAMP) is a major driver of cystogenesis in PKD[11]. Levels of cAMP are elevated in cyst epithelial cells from humans with ADPKD and in cystic kidneys from *Pkd1* and *Pkd2* mutant mice[12]. Elevated cAMP levels contribute to cyst growth by stimulating fluid secretion through activation of the CFTR chloride channel and by increasing cell proliferation through activation of the B-Raf/MEK/ERK pathway[13]. The mitogenic response to cAMP is inhibited by treatment with Ca^{2+} ionophores, whereas treatment with Ca^{2+} channel blockers stimulates proliferation. These results suggest that the effects of elevated cAMP are dependent on a reduction in intracellular Ca^{2+} concentration. Incubation of embryonic kidneys from *Pkd1* mutant mice with 8-Br-cAMP stimulates cyst formation[14]. Conversely, drugs that reduce intracellular cAMP levels, such as tolvaptan and octreotide, inhibit cyst growth in *Pkd1* and *Pkd2* mutant mice[15]. Clinical trials have shown that tolvaptan and octreotide reduce the rate of kidney enlargement and/or slow the decline in GFR in humans with ADPKD. Tolvaptan is now approved for the treatment of ADPKD in some countries, although it has not been approved for this indication in the United States[16].

The mechanism whereby cAMP is elevated in PKD remains poorly understood. cAMP is synthesized from ATP by adenylyl cyclases and is catabolyzed by phosphodiesterases. Intracellular cAMP signaling is tightly compartmentalized by A-kinase anchoring proteins (AKAPs) that bind to adenylyl cyclases, protein kinase A, and phosphodiesterase, thereby maintaining protein kinase A in close proximity to enzymes that synthesize and degrade cAMP. Our previous studies have revealed that renal cilia contain a cAMP-regulatory complex comprising adenylyl cyclases 5 and 6 (AC5/6), A-kinase anchoring protein 150 (AKAP150), protein kinase A, and phosphodiesterase 4C (PDE4C)[17]. The formation of this protein complex is disrupted in *Kif3a* mutant cells that lack primary cilia, which results in elevations in cAMP levels and activation of cAMP-dependent signaling both in vitro and in vivo. Moreover, we showed that PC2 interacts with the complex by binding to AC5/6 through its C-terminus. Ablation of PC2 increases cAMP levels, which can be corrected by re-expression of wild-type PC2 but not by mutant PC2 that lacks calcium channel activity. Since AC5/6 are Ca^{2+}-sensitive adenylyl cyclases, these findings suggest that endogenous PC2 raises the local concentration of Ca^{2+}, which suppresses AC5/6 activity. Mutation of PC2 or disruption of cilia releases the inhibition of AC5/6 and causes the cAMP elevation that drives kidney cystogenesis. Treatment of *Kif3a* mutant cells with the AC5 inhibitor NKY80 or siRNA knockdown of AC5 mRNA attenuates the increase in cAMP-dependent signaling. In contrast, siRNA knockdown of AC6 has no effect. These results suggest that AC5 mediates the increase in cAMP levels in *Kif3a* mutant cells and kidneys.

To test the role of AC5 in an orthologous animal model of human PKD, we generated mutant mice that were deficient in both *Pkd2* and AC5. Compared with *Pkd2* single mutant mice, concomitant ablation of AC5 reduced kidney enlargement, lowered cyst index, and improved kidney function. Importantly, cAMP levels in the kidney were increased in *Pkd2* single mutant mice and were reduced in AC5/*Pkd2* double mutant mice. These findings demonstrate that AC5 contributes to the increase in cAMP observed in PKD and provide genetic proof of concept for inhibition of AC5 as a therapeutic approach in PKD.

RESULTS

Adenylyl cyclase 5 (AC5) contributes to the elevation in cAMP caused by deficiency of *Pkd2* in mouse kidney cells

Our previous studies showed that inhibition of AC5 attenuates cAMP-dependent signaling in *Kif3a*-deficient renal epithelial cells that lack primary cilia[17]. To examine the role of AC5 in an orthologous model of PKD, we performed studies on *Pkd2* mutant cells and kidneys. As shown previously[17], cAMP levels were elevated in homozygous null $Pkd2^{-/-}$ renal epithelial cells compared to $Pkd2^{+/-}$ cells (Fig. 1A, left panel). Similarly, cAMP levels were elevated in kidneys from Pkhd1/Cre;$Pkd2^{F/F}$ mice[18], in which *Pkd2* has been deleted in renal collecting ducts by Cre/loxP recombination (Fig. 1A, right panel). These results confirmed that deficiency of *Pkd2* increases cAMP levels in kidney cells. Quantitative RT-PCR showed that the levels of AC5 mRNA transcripts were 10-fold higher in kidneys from collecting duct-specific *Pkd2* knockout mice compared to their wild-type littermates (Fig. 1B). Immunoblot analysis with an AC5-specific antibody (501AP) showed increased levels of AC5 protein in *Pkd2* mutant cells compared to controls (Fig. 1C, upper panel).

Immunoblotting with an antibody (C17) that recognizes both AC5 and AC6 also showed increased protein abundance in *Pkd2* mutant cells (Fig. 1C, lower panel). We were unable to measure AC6 protein by itself since an antibody that was specific for this isoform was not available. To determine the contribution of AC5 to the elevation in cAMP levels, we first used siRNA to knockdown AC5 in *Pkd2*$^{-/-}$ renal epithelial cells. Compared with control cells transfected with scrambled siRNA, transfection with AC5 siRNA reduced the levels of AC5 mRNA transcripts by 50–60% (Fig. 1D). Fig. 1E shows that cAMP levels were elevated in *Pkd2* null cells, and knockdown of AC5 reduced cAMP levels by 70%. In contrast, knockdown of AC5 had no significant effect in *Pkd2*$^{+/-}$ cells. To address the role of AC6, we inhibited its expression in *Pkd2* null cells using siRNA. The magnitude of the inhibition of AC6 was similar to the siRNA knockdown of AC5 (Suppl. Fig. 1A). The inhibition of AC6 was specific, since the expression of AC5 was unaffected by the AC6 siRNA (Suppl. Fig. 1B). Similar to the effect of siRNA knockdown of AC5, knockdown of AC6 reduced cAMP levels in *Pkd2* null cells (Suppl. Fig. 1C). Combined knockdown of AC5 and AC6 did not produce an additional effect (not shown). We conclude that both AC5 and AC6 contribute to the elevation of cAMP levels in *Pkd2* mutant cells.

Knockout of AC5 slows cyst progression caused by collecting duct-specific deletion of *Pkd2*

To explore the role of AC5 in the formation of kidney cysts in vivo, we generated *Pkd2*/AC5 double knockout mice. For these experiments, we used AC5 null mice in which exon 2 of the AC5 gene (*Adcy5*) has been deleted by homologous recombination[19]. Homozygous null mice are globally deficient in AC5 but are healthy and have normal kidney size and histology ([19] and Fig. 2F). AC5 null mice were crossed with Pkhd1/Cre;*Pkd2*$^{F/+}$ mice, and the progeny were intercrossed to generate *Pkd2* single knockout mice (SKO, AC5$^{+/+}$;*Pkd2*$^{F/F}$;Pkhd1/Cre) and *Pkd2*/AC5 double knockout mice (DKO, AC5$^{-/-}$;*Pkd2*$^{F/F}$;Pkhd1/Cre). The genotype of double knockout mice determined by genomic PCR is shown in Fig. 2A, in which the 450-bp wild-type AC5 product has been replaced with a 650-bp deletion product, and 450-bp *Pkd2*$^{F/F}$ and 235-bp Pkhd1/Cre products are also present. Quantitative RT-PCR analysis confirmed the absence of AC5 mRNA transcripts in DKO mouse kidneys (Fig. 2B, left panel). To confirm the absence of AC5 protein, we performed immunoblot analysis using an AC5-specific antibody (Fig. 2B, right panel). In lysates from *Pkd2* SKO kidneys, we detected the 140-kDa predicted protein as well as higher molecular weight species that likely represent glycosylated forms of the protein, as previously observed in other tissues[20]. Immunoblot analysis confirmed the absence of both the 140-kDa protein and the higher molecular weight species in lysates from *Pkd2*/AC5 DKO kidneys (Fig. 2B). To identify the cell types that express AC5 in the kidney, we performed indirect immunofluorescence with the anti-AC5 antibody. In the renal medulla of wild-type mice, AC5 protein was detected in renal tubules, including DBA-positive collecting ducts (Fig. 2C). In *Pkd2* SKO mice, AC5 was present in the epithelium of cystic collecting ducts and surrounding tubules. In contrast, homozygous null AC5$^{-/-}$ mice and AC5/*Pkd2* DKO mice showed only background staining.

Pkhd1/Cre;*Pkd2*$^{F/F}$ mice (SKO) developed cysts in renal collecting ducts beginning at postnatal day 8 (P8) followed by rapid cyst progression and kidney enlargement[18]. As shown

in Fig. 2D, cysts in DBA-positive collecting ducts were present in kidneys from AC5$^{+/+}$;*Pkd2*$^{F/F}$;Pkhd1/Cre mice (SKO) and AC5$^{-/-}$;*Pkd2*$^{F/F}$;Pkhd1/Cre (DKO) mice at P14. However, the cystic kidney disease in *Pkd2*/AC5 DKO mice was less severe than in *Pkd2* SKO mice (Fig. 3D), which was reflected by a 30% reduction in kidney weight (Fig. 2E). To further quantify cyst formation, we measured the cyst index in kidneys from SKO and DKO mice at P14. As shown in Fig. 3A, the cyst index was significantly reduced by 25% in DKO kidneys compared to SKO kidneys at the same age. The average size of cysts was also reduced by 31% in DKO kidneys compared to SKO kidneys, whereas the number of cysts was not significantly different (Fig. 3B–C). These findings suggest that deficiency of AC5 inhibits cyst expansion and kidney enlargement in *Pkd2* mutant mice but may not affect cystogenesis *per se*. To determine the effects on renal function, we measured serum creatinine using a sensitive and specific capillary electrophoresis method. Deficiency of AC5 by itself had no effect on serum creatinine (Fig. 3E). *Pkd2* SKO mice showed impaired kidney function at P14 as evidenced by elevated serum creatinine. The elevation in creatinine was substantially prevented in *Pkd2*/AC5 DKO mice. Renal expression of kidney injury marker 1 (*Kim1*) and neutrophil gelatinase-associated lipocalin (*Ngal*) was also reduced by about 50% in DKO mice compared to SKO mice (Fig. 3F) providing additional evidence that AC5 deficiency is protective against renal injury in this model of PKD.

Knockout of AC5 reduces renal cAMP levels and inhibits cAMP-dependent signaling in *Pkd2* mutant mice

Since AC5 mediates the synthesis of cAMP from ATP, we compared the cAMP content in the kidneys of *Pkd2* SKO mice and AC5/*Pkd2* DKO mice at P14. As shown previously (Fig. 1A), cAMP levels were 7-fold higher in AC5$^{+/+}$;*Pkd2*$^{F/F}$;Pkhd1/Cre (*Pkd2* SKO) kidneys than that in wild-type kidneys (Fig. 4A). Importantly, renal cAMP levels were reduced by 70% in AC5$^{-/-}$;*Pkd2*$^{F/F}$;Pkhd1/Cre (AC5/*Pkd2* DKO) littermates at the same age. These results reveal that upregulation of AC5 significantly contributes to the elevation in cAMP in *Pkd2* mutant mice. However, ablation of AC5 did not completely restore cAMP levels to wild-type levels, possibly due to the contribution of other adenylyl cyclases, such as AC6 or AC3[21].

To confirm the mechanism whereby ablation of AC5 reduces cyst growth, we measured cAMP-dependent signaling in *Pkd2* SKO mice and AC5/*Pkd2* DKO mice. Intracellular cAMP binds to the regulatory subunit of inactive protein kinase A (PKA) releasing the active catalytic subunit that phosphorylates downstream proteins. Among the known proteins that are phosphorylated by PKA in the kidney is the transcription factor CREB (cAMP-response element binding protein). Thus, CREB phosphorylation on Ser-133 is a readout of cAMP signaling in vivo. Immunoblot analysis with an antibody that specifically recognizes phospho-Ser-133 showed that levels of pCREB were increased in *Pkd2* SKO mice compared to wild-type mice and were decreased in AC5/*Pkd2* DKO mice compared to *Pkd2* SKO mice (Fig. 4B). Similarly, immunoblot analysis with an antibody that recognizes phosphorylated PKA substrates (PKA-S1) showed increased protein phosphorylation in SKO mice compared to wild-type mice and decreased phosphorylation in DKO mice compared to SKO mice. Quantification of band intensity showed that pCREB was increased about 60% in *Pkd2* SKO kidneys compared with wild-type kidneys. Concomitant AC5 knockout reduced

pCREB by about 25%, although this reduction did not achieve statistical significance(Fig. 4C, left panel). Phosphorylation of PKA substrates was increased about 90% in *Pkd2* SKO kidneys and was reduced about 80% in AC5/*Pkd2* DKO kidneys (Fig.4C right). To confirm that these changes occurred in the cyst epithelium, we performed immunofluorescence with antibodies specific for pCREB and phosphorylated PKA substrates. Immunofluorescence showed nuclear staining of DBA-positive cyst epithelial cells in kidneys from *Pkd2* SKO mice that was reduced in AC5/*Pkd2* DKO littermates (Fig. 4D). Quantification of fluorescence intensity showed that pCREB staining was reduced by 98% in AC5/*Pkd2* DKO collecting ducts compared to *Pkd2* SKO collecting ducts (P=0.0003, n=3). The staining of phosphorylated PKA substrates showed a statistically non-significant reduction of 56% (P=0.13, n=3).

Knockout of AC5 reduces ciliary elongation in *Pkd2* mutant mice

We previously identified AC5 and AC6 in a complex with AKAP150 and PC2 in primary cilia in kidney cells. Because the antibody used in prior studies (C-17) did not distinguish between AC5 and AC6, we were unable to determine which of the isoforms is endogenously expressed in renal cilia. Using an antibody specific for AC5 that is now available (PAC-501AP), we examined the expression of endogenous AC5 in kidney cells. Indirect immunofluorescence showed that endogenous AC5 co-localized with acetylated α-tubulin in the primary cilia of renal tubular cells in the kidney (Fig. 5B). The specificity of the ciliary staining was validated by immunofluorescence on AC5 null kidneys (Suppl. Fig. 2A). AC5 was also located in the cell body. To confirm the localization in primary cilia, we performed subcellular fractionation. Immunoblot analysis detected endogenous AC5 in subcellular fractions containing acetylated α-tubulin, a marker of primary cilia (Fig 5A). Immunoblotting with the C17 antibody confirmed that AC5 and/or AC6 were present in ciliary fractions. Although an AC6-specific antibody is not available, Suppl. Fig. 2B shows that the C17 antibody stained primary cilia in $AC5^{-/-}$ mice, suggesting that AC6 was also present in primary cilia. Collectively, these findings support the existence of a cAMP-regulatory complex containing AC5 and AC6 in renal cilia.

Elevations in intracellular cAMP levels are associated with elongation of the primary cilium[22], a sensory organelle that plays a central role in the pathogenesis of PKD and other ciliopathies. Although the mechanism of ciliary elongation is poorly understood, ciliary length serves as an additional readout of cAMP levels and may be relevant to cyst progression. We stained the primary cilia in renal collecting ducts with an antibody against ARL13B and quantified cilia length using 3D images and the method described by Saggese[23]. As shown in Fig. 5C, we observed that cilia in AC5 null collecting ducts were shorter than in wild-type collecting ducts. The average cilium length was 3.2 μm in wild-type kidneys and 2.2 μm in AC5-deficient kidneys (Fig. 5D). In *Pkd2* SKO kidneys the cilium length was increased to 4.9 μm, consistent with the increase in cAMP levels. Ciliary length was reduced to 2.5 μm in *Pkd2*/AC5 DKO kidneys. Thus, concomitant ablation of AC5 restores normal ciliary length in *Pkd2* mutant kidneys correlating with the reduction in cAMP levels.

DISCUSSION

Intracellular levels of cAMP are reciprocally regulated by the activities of adenylyl cyclases (ACs) and phosphodiesterases (PDEs). Mammals express nine membrane-associated ACs (AC1–AC9) and one soluble AC (sAC), which differ in their tissue distribution, subcellular localization, and regulation[24]. All membrane-associated ACs are stimulated by GTP-bound $G\alpha_s$, which is formed when ligand binding activates G protein-coupled receptors (GPCRs) that catalyze the exchange of GDP with GTP on the α subunit of heterotrimeric G proteins. Activated $G\alpha_s$ dissociates from Gβγ subunits and interacts with and stimulates ACs. The activity of membrane-associated ACs can also be regulated by Ca^{2+}/calmodulin, inhibitory G proteins, Gβγ subunits, cytosolic Ca^{2+}, protein phosphorylation, and phosphoinositides. Among the nine membrane-bound ACs, mRNA transcripts encoding AC5 and AC6 have been identified in renal collecting ducts[25], and upregulation of AC5 and AC6 has been detected in human ADPKD cells[21]. In addition, cyst fluid from ADPKD kidneys contains a lipid with properties similar to forskolin, a diterpene that stimulates AC activity[26]. The membrane-bound ACs can be classified based on their regulation by Ca^{2+}/calmodulin and cytosolic Ca^{2+}. AC5 and AC6 are uniquely inhibited by sub-micromolar concentrations of Ca^{2+}. We previously showed that AC5 and AC6 are located in primary cilia in renal epithelial cells, and cAMP levels are elevated in cystic kidneys from *Kif3a* mutant mice, a non-orthologous animal model of PKD in which loss of renal cilia causes kidney cysts[17]. Treatment with the AC5 inhibitor NKY80 or siRNA silencing of AC5 (but not AC6) reduced cAMP-dependent signaling in *Kif3a* mutant renal epithelia cells. These results suggested that AC5 mediates the increase in cAMP in cystic kidneys in *Kif3a* mutant mice.

In this study we tested the role of AC5 in an orthologous animal model of PKD produced by mutations of *Pkd2*. Mutations of *PKD2* are responsible for 15–20% of the cases of ADPKD[1]. Kidney-specific ablation of the orthologous mouse *Pkd2* gene produces kidney cysts, enlarged kidneys, and renal failure[10]. We found that AC5 mRNA is increased in cystic kidneys from mice with collecting-duct-specific ablation of *Pkd2*. This finding is consistent with prior studies by Pinto et al. showing increased expression of AC5 in human ADPKD[21]. Here, we showed that both in vitro knockdown and in vivo knockout of AC5 attenuated the elevation in cAMP caused by deletion of *Pkd2* in renal tubular cells. AC5/*Pkd2* double knockout mice exhibited lower kidney/body weight ratio, reduced cyst index, and smaller average cyst size compared with *Pkd2* single knockout mice. As a consequence, kidney injury was reduced as evidenced by lower serum creatinine and reduced expression of Ngal and Kim-1. Although the salutary effects of AC5 deficiency on cyst growth were relatively modest, over the lifespan of an individual a 25–30% reduction in cyst index and total cyst area may be sufficient to delay or prevent progression to end-stage renal disease. To assess the longer-term effects of AC5 knockout, further studies would need to be performed using a more slowly progressive mouse model, such as $Pkd2^{WS25/-}$ [27].

Previous studies have shown that cystogenesis in *Pkd1* mutant mice is reduced by ablation of AC6, an isoform of adenylyl cyclase that is closely related to AC5[28]. Deletion of AC6 in renal collecting ducts using AQP2-Cre mice decreased kidney size and reduced cystogenesis in *Pkd1* mutant mice. Here, we showed that knockdown of either AC5 or AC6 decreases cAMP levels in *Pkd2* null kidney cells. Genetic ablation of AC5 lowers renal cAMP levels

and reduces cAMP-dependent phosphorylation in *Pkd2* mutant kidneys. Taken together, these results suggest that both AC5 and AC6 contribute to the cAMP elevation caused by mutation of *Pkd2* in the kidney. Knockout of AC5 did not completely restore cAMP levels to normal, presumably reflecting continued activity of AC3 and AC6, which are also upregulated in PKD. Additional studies will be needed to determine whether combined ablation of AC5 with AC6 or AC3 further improves renal cystic disease.

In addition to kidney cysts, ADPKD is characterized by the formation of cysts in other organs including the liver. Liver cysts arise from intrahepatic bile ducts and can cause massive hepatomegaly but generally do not cause hepatic failure. Spirli et al. have recently shown that knockout of AC5 reduces cAMP levels in *Pkd2*-deficient cholangiocytes and slows the growth of biliary cysts in cultured hepatic organoids[29]. Pharmacological inhibition of AC5 decreased liver enlargement in *Pkd2* mutant mice. In contrast, deficiency of AC6 did not significantly reduce cAMP levels or inhibit the growth of liver cysts. Our studies show that genetic ablation of AC5 reduces renal cAMP levels, slows the growth of kidney cysts, and improves kidney function in *Pkd2* knockout mice. Collectively, these findings suggest that AC5 may play a more general role in cyst growth and identify AC5 as a potential therapeutic target for slowing the growth of kidney and liver cysts in PKD.

We previously identified AC5/6 in a multiprotein complex in the primary cilium of renal epithelial cells[17]. Because the antibody used in previous studies recognized both AC5 and AC6, we were unable to distinguish which of these isoforms was endogenously expressed in renal cilia. In the current study we used a newly available AC5-specific antibody to localize endogenous AC5 in the kidney. The specificity of the antibody was verified by immunoblot analysis, which showed the absence of immunoreactivity in AC5-knockout mice. Indirect immunofluorescence showed that endogenous AC5 was located in renal cilia in wild-type kidneys but was not detected in the cilia of AC5 null kidneys. Sucrose density gradient centrifugation showed that endogenous AC5 was present in fractions containing the ciliary markers acetylated α-tubulin and IFT140 as well as PC2, AKAP150, PKA, and epitope-tagged PDE4C. These studies confirm the existence of a cAMP-regulatory complex in renal cilia and identify AC5 as a component of the complex. AC6 also appears to be located in renal cilia. The interaction of PC2 with the Ca^{2+}-sensitive isoform AC5 suggests that Ca^{2+} entry via PC2 may function to inhibit AC5. cAMP levels would be further constrained by the presence of PDE4C in the complex. Consistent with this model, Moore et al. recently showed, using novel cilia-targeted sensors, that cAMP levels and PKA activity are maintained at tonically elevated levels in primary cilia through the activities of AC5/6[30]. Their studies also showed that sonic hedgehog activates a Ca^{2+} channel, possibly PC2, which raises local Ca^{2+} concentration and inhibits AC5/6 resulting in a lowering of cAMP levels.

Increased generation of cAMP in the ciliary compartment is unlikely to account for the elevation of cAMP in *Pkd2* mutant cells and kidneys, since the volume of the primary cilium is 1/5,000 of the volume of the cell body[31]. However, it is known that a small change in ciliary cAMP can induce dramatic signaling events in the cell body. For example, mating of *Chlamydomonas* gametes is triggered by flagellar adhesion and activation of a flagellar (ciliary) adenylyl cyclase that results within minutes in a >15-fold elevation in cAMP in the

cell body[32, 33]. An analogous mechanism may underlie the regulation of cAMP in kidney tubule cells.

Another important finding was that the length of renal cilia is regulated by AC5 in vivo. Besschetnova et al.[22] first showed that elevations in cAMP and subsequent PKA activation increase the length of primary cilia in IMCD renal epithelial cells. Conversely, cilia are shortened by PKA inhibitors. Blocking Ca^{2+} entry or release from intracellular stores also increase cAMP levels and result in cilia elongation. The mechanism of cAMP-dependent cilia elongation is not known but may involve accelerated anterograde IFT. siRNA-mediated knockdown of AC5 and AC6 blocked ciliary elongation induced by Gd^{3+}, suggesting that these isoforms of adenylyl cyclase are involved. Here, we showed that knockout of *Pkd2* in renal collecting ducts resulted in elongation of primary cilia, consistent with the increase in cAMP levels. Concomitant ablation of AC5 in AC5/*Pkd2* DKO mice normalized cilia length in association with an improvement in kidney structure and function. Cilium length is dynamically regulated by intraflagellar transport machinery through PKA, aurora-A, NIMA, Tectex-1, Nedd9, PIPO, VHL, NDE, CaMKII and IPP5E, and increased cilia length has previously been observed in several animal models of cystic kidney disease, including NPHP, MKS, BBS, and $Pkd1^{RC/RC}$ mice[34]. Treatment of *jck* mice, a model of nephronophthisis, with R-roscovitine reduces ciliary length and decreases the severity of cystic kidney disease[35]. Ablation of cilia via inactivation of genes that encode proteins required for IFT suppresses cyst growth in mice with conditional inactivation of *Pkd1* or *Pkd2*, revealing the existence of a cilia-dependent factor that stimulates cystogenesis[10]. Taken together, these studies suggest that the decrease in cilia length in AC5/*Pkd2* double knockout mice may suppress a ciliary cyst-activating factor resulting in a reduction in cyst severity.

Our results provide genetic proof of concept for inhibition of AC5 as a potential treatment for kidney cysts in PKD. AC5-deficient mice exhibit normal organ histology, longer lifespan, and protection from cardiomyopathy and cancer[19, 36–38], suggesting that inhibition of AC5 might have salutary effects. However, Parkinson-like motor dysfunction, reduced ethanol sensitivity, and neurobehavioral abnormalities have also been reported[38–40]. Further studies will be needed to assess the therapeutic potential and tolerability of AC5 inhibitors in PKD.

METHODS

Cell culture and siRNA transfection

Mouse $Pkd2^{+/-}$ and $Pkd2^{-/-}$ renal epithelial cell lines were described previously[41]. Cells were grown in DMEM/F12 supplemented with 1.3 μg/ml sodium selenite (Sigma), 5 μg/ml insulin (Sigma), 5 μg/ml transferrin (Sigma), 1 μg/ml 3,3,5'-triiodo-L-thyronine (Sigma), 2% FBS and 0.1 unit/ml IFNγ at 33°C as described previously[17]. Cells were transfected with 50 nM control siRNA or AC5-specific siRNA (Dharmacon) using Lipofectamine 2000 (Invitrogen) according to the manufacturer's directions. After 48 h, the cells were harvested and used for cAMP assay, RNA isolation, and protein analysis.

Protein fractionation and immunoblot analysis

Pkd2$^{+/-}$ cells were transfected with PDE4C-Flag[17] then incubated at room temperature for 30 min in protein extraction buffer containing 50 mM Tris-Cl, 150 mM NaCl, 5 mM EDTA, 0.1% Triton X-100, 0.1% deoxycholic acid, 100 mM PMSF, and 1 tablet/10 ml protease inhibitor cocktail (Roche, Indianapolis, IN). Extracts were clarified by centrifugation at 12,000×*g* for 10 min, and the supernatant was fractionated by ultracentrifugation through a 5–40% sucrose gradient at 4°C for 3 h. Fourteen fractions were collected from the top of the gradient, and 15 μl of each fraction was mixed with 2×SDS sample buffer (Bio-Rad). SDS-PAGE analysis was performed with 4–15% Nu-PAGE gels. Proteins were transferred to nylon membranes, and immunoblot analysis was performed with antibodies against markers of Golgi (GM130, Sigma), endoplasmic reticulum (calnexin, Sigma), plasma membrane (CD44, Sigma), and primary cilia [acetylated α-tubulin, Sigma; intraflagellar protein 140 (IFT140), gift from Dr. William Snell, UT Southwestern]. Additional antibodies were directed against polycystin-2 (YCC2), AC5/6 (C17, Santa Cruz), AC5 (PAC-501AP, FabGennix), AKAP150 (Santa Cruz), PKA-RIIa (BD Transduction Laboratories), pCREB and phosphorylated PKA substrates (Cell Signaling).

cAMP assays

cAMP levels in cells and kidneys were measured using Direct cAMP ELISA kits (Enzo) according to the manufacturer's directions. Briefly, cells and flash-frozen tissue were lysed in 0.1 M HCl. After centrifugation, the supernatant was added to wells coated with goat anti-rabbit IgG followed by a solution of cAMP-conjugated to alkaline phosphatase and rabbit anti-cAMP antibody. After incubation for 2 h at room temperature, the substrate p-nitrophenylphosphate was added, and the colorimetric reaction product was measured after 1 h using a SynergyHT plate reader (BioTeck) at 405 nm. cAMP concentration was normalized to protein concentration measured with the Micro BCA Protein Assay Kit (Pierce).

Animal studies

AC5 knockout mice were described previously[19]. AC5$^{+/-}$ mice were crossed with AC5$^{+/+}$;*Pkd2*$^{F/+}$;Pkhd1/Cre mice[18], and the progeny (AC5$^{+/-}$;*Pkd2*$^{F/+}$;Pkhd1/Cre) were intercrossed to generate *Pkd2* single knockout mice (SKO, AC5$^{+/+}$;*Pkd2*$^{F/F}$;Pkhd1/Cre) and *Pkd2*/AC5 double knockout mice (AC5$^{-/-}$;*Pkd2*$^{F/F}$;Pkhd1/Cre). Genotypes were determined by PCR using the following primers: AC5 wild-type: forward primer 5′-ACCGTCGAGGATGGAGACGG-3′; reverse primer 5′-GTGGCTGTGGCAGCAACAGG-3′. The DNA fragment size is 450 bp. AC5 deletion: Forward primer 5′- ACCGTCGAGGATGGAGACGG-3′; reverse primer 5′-CAGCGCGGCAGACGTGCGCT-3′. The DNA fragment size is 650 bp. *Pkd2* primers and Pkhd1/Cre primers were the same as in published papers[42]. Genomic DNA was extracted from tail biopsies of 1-week old mice according to the kit instructions (Direct Tail Digestion, Viagen Biotech). PCR was then carried out for 35 cycles at 94°C for 30 s, 58°C for 30 s, and 68°C for 1 min with GoTaq Green Master Mix (Promega). All experiments involving animals was approved by the University of Texas Southwestern and University of Minnesota

Institutional Animal Care and Research Advisory Committees. Animals of both sexes were used in experiments. The genetic background was C57BL/6.

Histology and immunofluorescence

For histological analysis, mice were anesthetized according to approved protocols and perfused with ice-cold PBS and 4% (wt/vol) paraformaldehyde. Kidneys were harvested, incubated at 4°C overnight and embedded in paraffin. 2 μm-thick sagittal kidney sections were mounted, stained with hematoxylin and eosin (H&E), and examined by light microscopy. All kidneys were photographed under the same magnification using an ArtixScan-4000ft (MicroTek). ImageJ software was used to calculate the cyst index, cyst size, and cyst number. Cyst index was calculated as the cumulative area of cysts divided by the total area of the kidney. For indirect immunofluorescence, kidney tissues were fixed with 4% paraformaldehyde and embedded in paraffin or cryoprotected with 10% sucrose, frozen, and embedded in OCT (Fisher). 5 μm-thick sagittal sections were used for immunostaining with antibodies against AC5 (1:100; PAC-501AP, FabGennix Inc.), pCREB (1:400, Cell Signaling), p-PKA substrates (1:400), acetylated α-tubulin (1:1000, Sigma), or ARL13B(1:400, Proteintech). Secondary antibodies were conjugated to Alexa Fluor-488 or Alexa Fluor-594 (Molecular Probes, Eugene, OR). Lectin staining was performed using FITC-coupled *Dolichos biflorus* agglutinin (DBA, Vector Laboratories, Burlingame, CA). The stained sections were mounted with Prolong Gold antifade reagent containing DAPI (Life Technologies). Images were acquired using a Zeiss Axioplan2 deconvolution microscope with AxioVision software.

Real-time RT-PCR

Total RNA was isolated from kidneys and cells using TRIzol reagent according to the manufacturer's protocol (Invitrogen). cDNAs were synthesized using the iScript first- strand synthesis system (Bio-Rad) and then amplified by PCR with transcript-specific primers for AC5, Ngal and Kim1[43]. Real-time PCR was performed in triplicate using CFX Connect Real-Time system and SYBR green Supermix reagents (Bio-Rad Laboratories, Hercules, CA). 18S rRNA was used as the control gene for normalization. Data were analyzed using Prism 6.

Cilium length measurement

Kidney sections were stained with antibodies against ARL13B or acetylated α-tubulin and imaged using a Zeiss LSM510 confocal microscope with Zenlite software. Z-stack images were processed in ImageJ following the method described by Saggese[23]. 3D reconstructions were made from Z-stack images, and the length of the primary cilium was quantified using the 3D subject count plugin.

Statistical analysis

Experiments were performed with 3–5 biological replicates. Statistical analysis was performed using two-tailed unpaired Student's *t* test. For multiple comparisons, ANOVA and Dunnett's post hoc test of significance were performed using GraphPad Prism 6 software. $P<0.05$ was considered statistically significant.

Supplementary Material

Refer to Web version on PubMed Central for supplementary material.

Acknowledgments

Research reported in this publication was supported by the National Institutes of Health under award number R37DK042921 (P.I.) and the UT Southwestern O'Brien Kidney Research Core Center (P30DK079328). The content is solely the responsibility of the authors and does not necessarily represent the official views of the National Institutes of Health. We thank Drs. Kirk Hammond and Tong Tang (University of California, San Diego) for providing the AC5 knockout mice, Dr. William Snell (UT Southwestern) for the antibody against IFT140, Dr. Karam Aboudehen (University of Minnesota) for critically reviewing the manuscript, the UT Southwestern Live Cell Imaging Core Facility for image analysis, and Matanel Yheskel for expert technical assistance.

Dr. Vishal Patel is a consultant and receives grant support from Regulus Therapeutics.

References

1. Igarashi P, Somlo S. Genetics and pathogenesis of polycystic kidney disease. J Am Soc Nephrol. 2002; 13:2384–2398. [PubMed: 12191984]
2. Pazour GJ, San Agustin JT, Follit JA, et al. Polycystin-2 localizes to kidney cilia and the ciliary level is elevated in orpk mice with polycystic kidney disease. Curr Biol. 2002; 12:R378–R380. [PubMed: 12062067]
3. Yoder BK, Hou X, Guay-Woodford LM. The polycystic kidney disease proteins, polycystin-1, polycystin-2, polaris, and cystin, are co-localized in renal cilia. J Am Soc Nephrol. 2002; 13:2508–2516. [PubMed: 12239239]
4. Nauli SM, Alenghat FJ, Luo Y, et al. Polycystins 1 and 2 mediate mechanosensation in the primary cilium of kidney cells. Nat Genet. 2003; 33:129–137. [PubMed: 12514735]
5. Delling M, Indzhykulian AA, Liu X, et al. Primary cilia are not calcium-responsive mechanosensors. Nature. 2016; 531:656–660. [PubMed: 27007841]
6. O'Connor AK, Malarkey EB, Berbari NF, et al. An inducible CiliaGFP mouse model for in vivo visualization and analysis of cilia in live tissue. Cilia. 2013; 2:8. [PubMed: 23819925]
7. Raychowdhury MK, Ramos AJ, Zhang P, et al. Vasopressin receptor-mediated functional signaling pathway in primary cilia of renal epithelial cells. Am J Physiol Renal Physiol. 2009; 296:F87–97. [PubMed: 18945824]
8. Hogan MC, Manganelli L, Woollard JR, et al. Characterization of PKD protein-positive exosome-like vesicles. J Am Soc Nephrol. 2009; 20:278–288. [PubMed: 19158352]
9. Lin F, Hiesberger T, Cordes K, et al. Kidney-specific inactivation of the KIF3A subunit of kinesin-II inhibits renal ciliogenesis and produces polycystic kidney disease. Proc Natl Acad Sci U S A. 2003; 100:5286–5291. [PubMed: 12672950]
10. Ma M, Tian X, Igarashi P, et al. Loss of cilia suppresses cyst growth in genetic models of autosomal dominant polycystic kidney disease. Nat Genet. 2013; 45:1004–1012. [PubMed: 23892607]
11. Calvet JP. Strategies to inhibit cyst formation in ADPKD. Clin J Am Soc Nephrol. 2008; 3:1205–1211. [PubMed: 18434615]
12. Torres VE, Harris PC. Mechanisms of Disease: autosomal dominant and recessive polycystic kidney diseases. Nat Clin Pract Nephrol. 2006; 2:40–55. quiz 55. [PubMed: 16932388]
13. Yamaguchi T, Nagao S, Wallace DP, et al. Cyclic AMP activates B-Raf and ERK in cyst epithelial cells from autosomal-dominant polycystic kidneys. Kidney Int. 2003; 63:1983–1994. [PubMed: 12753285]
14. Magenheimer BS, St John PL, Isom KS, et al. Early embryonic renal tubules of wild-type and polycystic kidney disease kidneys respond to cAMP stimulation with cystic fibrosis transmembrane conductance regulator/Na(+),K(+),2Cl(−) Co-transporter-dependent cystic dilation. J Am Soc Nephrol. 2006; 17:3424–3437. [PubMed: 17108316]

15. Patel V, Chowdhury R, Igarashi P. Advances in the pathogenesis and treatment of polycystic kidney disease. Curr Opin Nephrol Hypertens. 2009; 18:99–106. [PubMed: 19430332]
16. Torres VE, Harris PC. Strategies targeting cAMP signaling in the treatment of polycystic kidney disease. J Am Soc Nephrol. 2014; 25:18–32. [PubMed: 24335972]
17. Choi YH, Suzuki A, Hajarnis S, et al. Polycystin-2 and phosphodiesterase 4C are components of a ciliary A-kinase anchoring protein complex that is disrupted in cystic kidney diseases. Proc Natl Acad Sci U S A. 2011; 108:10679–10684. [PubMed: 21670265]
18. Nishio S, Tian X, Gallagher AR, et al. Loss of oriented cell division does not initiate cyst formation. J Am Soc Nephrol. 2010; 21:295–302. [PubMed: 19959710]
19. Lee KW, Hong JH, Choi IY, et al. Impaired D2 dopamine receptor function in mice lacking type 5 adenylyl cyclase. J Neurosci. 2002; 22:7931–7940. [PubMed: 12223546]
20. Wang SC, Lai HL, Chiu YT, et al. Regulation of type V adenylate cyclase by Ric8a, a guanine nucleotide exchange factor. Biochem J. 2007; 406:383–388. [PubMed: 17593019]
21. Pinto CS, Reif GA, Nivens E, et al. Calmodulin-sensitive adenylyl cyclases mediate AVP-dependent cAMP production and Cl- secretion by human autosomal dominant polycystic kidney cells. Am J Physiol Renal Physiol. 2012; 303:F1412–1424. [PubMed: 22952279]
22. Besschetnova TY, Kolpakova-Hart E, Guan Y, et al. Identification of signaling pathways regulating primary cilium length and flow-mediated adaptation. Curr Biol. 2010; 20:182–187. [PubMed: 20096584]
23. Saggese T, Young AA, Huang C, et al. Development of a method for the measurement of primary cilia length in 3D. Cilia. 2012; 1:11. [PubMed: 23351171]
24. Duman, RS., Nestler, EJ. Cyclic Nucleotides. In: Siegel, GJ.Agranoff, BW.Albers, RW.Fisher, SK., et al., editors. Basic Neurochemistry: Molecular, Cellular and Medical Aspects. 6. Lippincott-Raven; Philadelphia: 1999.
25. Chabardes D, Firsov D, Aarab L, et al. Localization of mRNAs encoding Ca2+-inhibitable adenylyl cyclases along the renal tubule. Functional consequences for regulation of the cAMP content. J Biol Chem. 1996; 271:19264–19271. [PubMed: 8702608]
26. Putnam WC, Swenson SM, Reif GA, et al. Identification of a forskolin-like molecule in human renal cysts. J Am Soc Nephrol. 2007; 18:934–943. [PubMed: 17251383]
27. Wu G, D'Agati V, Cai Y, et al. Somatic inactivation of Pkd2 results in polycystic kidney disease. Cell. 1998; 93:177–188. [PubMed: 9568711]
28. Rees S, Kittikulsuth W, Roos K, et al. Adenylyl cyclase 6 deficiency ameliorates polycystic kidney disease. J Am Soc Nephrol. 2014; 25:232–237. [PubMed: 24158982]
29. Spirli C, Mariotti V, Villani A, et al. Adenylyl cyclase 5 links changes in calcium homeostasis to cAMP-dependent cyst growth in polycystic liver disease. J Hepatol. 2017; 66:571–580. [PubMed: 27826057]
30. Moore BS, Stepanchick AN, Tewson PH, et al. Cilia have high cAMP levels that are inhibited by Sonic Hedgehog-regulated calcium dynamics. Proc Natl Acad Sci U S A. 2016; 113:13069–13074. [PubMed: 27799542]
31. Nachury MV. How do cilia organize signalling cascades? Phil Trans R Soc B. 2014; 369:20130465. [PubMed: 25047619]
32. Pan J, Snell WJ. Signal transduction during fertilization in the unicellular green alga, chlamydomonas. Cur Opin Microbiol. 2000; 3:596–602.
33. Saito T, Small L, Goodenough UW. Activation of adenylyl cyclase in Chlamydomonas reinhardtii by adhesion and by heat. J Cell Biol. 1993; 122:137–147. [PubMed: 8390999]
34. Ong AC. Primary cilia and renal cysts: does length matter? Nephrol Dial Transplant. 2013; 28:2661–2663. [PubMed: 23935132]
35. Husson H, Moreno S, Smith LA, et al. Reduction of ciliary length through pharmacologic or genetic inhibition of CDK5 attenuates polycystic kidney disease in a model of nephronophthisis. Hum Mol Genet. 2016; 25:2245–2255. [PubMed: 27053712]
36. Vatner SF, Park M, Yan L, et al. Adenylyl cyclase type 5 in cardiac disease, metabolism, and aging. Am J Physiol Heart Circ Physiol. 2013; 305:H1–8. [PubMed: 23624627]

37. De Lorenzo MS, Chen W, Baljinnyam E, et al. Reduced malignancy as a mechanism for longevity in mice with adenylyl cyclase type 5 disruption. Aging Cell. 2014; 13:102–110. [PubMed: 23957304]

38. Sadana R, Dessauer CW. Physiological roles for G protein-regulated adenylyl cyclase isoforms: insights from knockout and overexpression studies. Neurosignals. 2009; 17:5–22. [PubMed: 18948702]

39. Kim KS, Kim H, Baek IS, et al. Mice lacking adenylyl cyclase type 5 (AC5) show increased ethanol consumption and reduced ethanol sensitivity. Psychopharmacology (Berl). 2011; 215:391–398. [PubMed: 21193983]

40. Kim H, Lee Y, Park JY, et al. Loss of Adenylyl Cyclase Type-5 in the Dorsal Striatum Produces Autistic-Like Behaviors. Mol Neurobiol. 2016

41. Grimm DH, Cai Y, Chauvet V, et al. Polycystin-1 distribution is modulated by polycystin-2 expression in mammalian cells. J Biol Chem. 2003; 278:36786–36793. Epub 32003 Jul 36782. [PubMed: 12840011]

42. Williams SS, Cobo-Stark P, Hajarnis S, et al. Tissue-specific regulation of the mouse Pkhd1 (ARPKD) gene promoter. Am J Physiol Renal Physiol. 2014; 307:F356–368. [PubMed: 24899057]

43. Patel V, Li L, Cobo-Stark P, et al. Acute kidney injury and aberrant planar cell polarity induce cyst formation in mice lacking renal cilia. Hum Mol Genet. 2008; 17:1578–1590. [PubMed: 18263895]

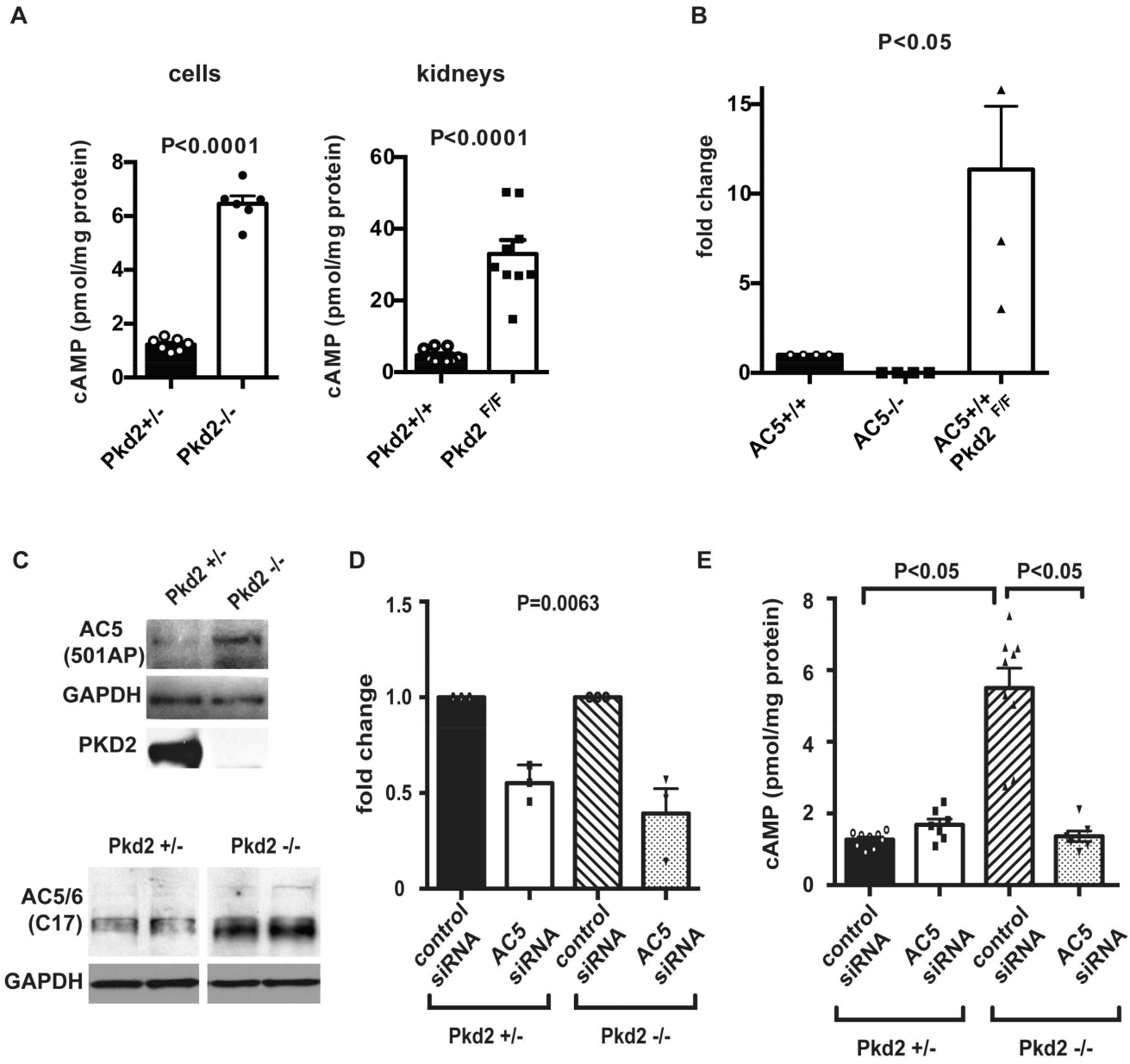

Figure 1. Adenylyl cyclase 5 (AC5) contributes to the elevation in cAMP caused by mutation of *Pkd2*

(**A**) cAMP levels are elevated in homozygous *Pkd2* null renal epithelial cells ($Pkd2^{-/-}$) compared with heterozygous $Pkd2^{+/-}$ cells (left panel). cAMP was measured in confluent cells and normalized to protein content. Results from six independent experiments are shown. Right panel shows that cAMP levels are elevated in kidneys from Pkhd1/Cre;$Pkd2^{F/F}$ mice compared with control Pkhd1/Cre;$Pkd2^{+/+}$ littermates (n=9). cAMP and protein concentration were measured at P14. Error bars represent SEM. (**B**) Expression of AC5 is increased in kidneys from Pkhd1/Cre;$Pkd2^{F/F}$ mice (open bar) compared with wild-type mice (filled bar). mRNA was extracted from kidneys at P14 (n=4), and levels of AC5 mRNA transcripts were measured by qRT-PCR and normalized to 18*S* rRNA. Expression is shown relative to wild-type kidneys ($AC5^{+/+}$). Middle bar shows absence of expression in kidneys

from homozygous null AC5$^{-/-}$ mice. Error bars represent SEM. (**C**) Immunoblot analysis with an AC5-specific antibody (501AP) and an antibody that recognizes both AC5 and AC6 (C17) shows increased expression in *Pkd2*$^{-/-}$ cells compared to *Pkd2*$^{+/-}$ cells. GAPDH was used as a loading control, and an antibody against polycystin-2 (PKD2) confirmed the absence of the protein in *Pkd2*$^{-/-}$ cells. (**D**) qRT-PCR shows reduction of AC5 mRNA levels in *Pkd2*$^{+/-}$ cells (left) and *Pkd2*$^{-/-}$ cells (right) transfected with AC5 siRNA (open bar, stippled bar) compared with cells treated with control siRNA (filled bar, hatched bar). Results from three independent experiments are shown. Error bars represent SEM. (**E**) Knockdown of AC5 reduces cAMP level in *Pkd2* null cells. cAMP levels are elevated in *Pkd2*$^{-/-}$ cells (hatched bar) compared to *Pkd2*$^{+/-}$ cells (filled bar). Knockdown of AC5 normalizes cAMP levels in *Pkd2*$^{-/-}$ cells (stippled bar) and has no significant effect in *Pkd2*$^{+/-}$ cells (open bar). Error bars represent SEM.

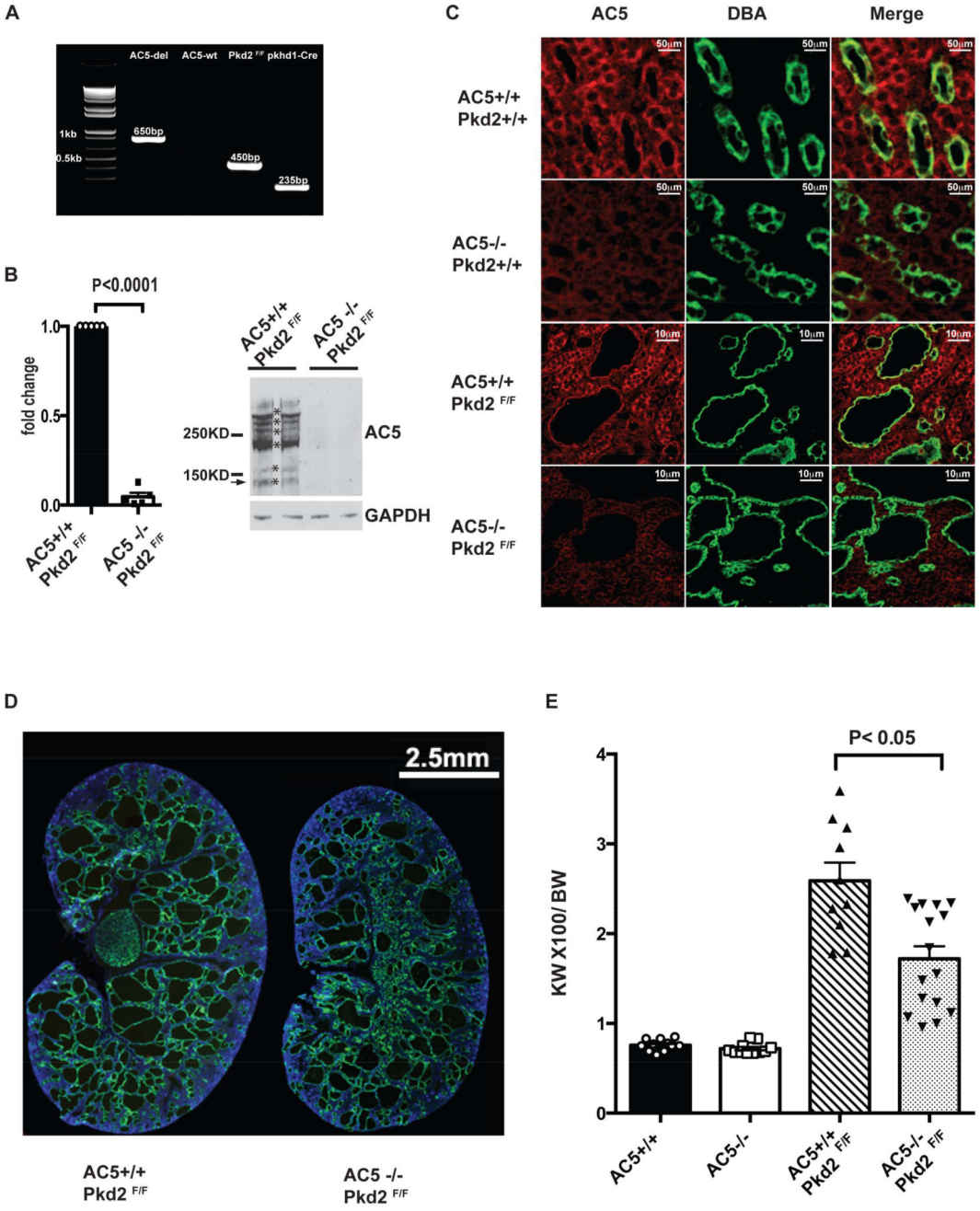

Figure 2. Knockout of AC5 in *Pkd2* mutant mice

(**A**) Genotyping of AC5$^{-/-}$, wild-type, *Pkd2*$^{F/F}$, and Pkhd1/Cre mice. Sequences of PCR primers are provided in the Materials and Methods. PCR amplification of tail DNA shows a 650-bp product that is specific for the AC5 deletion (lane 2) and is absent in wild-type mice (lane 3). Lane 4 shows the 450-bp *Pkd2*$^{F/F}$ product, and lane 5 shows the 235-bp Pkhd1/Cre product. (**B**) Left panel shows qRT-PCR analysis confirming the absence of AC5 mRNA transcripts in kidneys from AC5$^{-/-}$;*Pkd2*$^{F/F}$;Pkhd1/Cre mice (open bar) compared to AC5$^{+/+}$;*Pkd2*$^{F/F}$;Pkhd1/Cre controls (filled bar). Error bars represent SEM (n=5). Right panel shows immunoblot analysis of kidney lysates from AC5$^{-/-}$;*Pkd2*$^{F/F}$;Pkhd1/Cre mice

(right lanes) and AC5$^{+/+}$;*Pkd2*$^{F/F}$;Pkhd1/Cre controls (left lanes). Arrow indicates the predicted 140-kDa AC5 protein and * indicates higher molecular weight glycoforms that are present in controls and absent in AC5$^{-/-}$;*Pkd2*$^{F/F}$;Pkhd1/Cre mice. Lower panel shows GAPDH as a loading control. (**C**) Indirect immunofluorescence of kidneys from P14 mice with the indicated genotypes (all are Pkhd1/Cre-positive). Staining with anti-AC5 (501AP, 1:200) shows expression of AC5 (red) in renal tubules in AC5$^{+/+}$ mice and only background staining in AC5$^{-/-}$ mice. Co-staining with FITC-DBA (1:1,000, green) labels collecting ducts in *Pkd2*$^{+/+}$ mice and kidney cysts in *Pkd2*$^{F/F}$ mice. (**D**) Low magnification sagittal sections of P14 kidneys from AC5$^{+/+}$;*Pkd2*$^{F/F}$;Pkhd1/Cre mice (left) and AC5$^{-/-}$;*Pkd2*$^{F/F}$;Pkhd1/Cre mice (right) stained with FITC-DBA (green, 1:1,000) shows that renal cysts are derived from DBA-positive collecting ducts. Nuclei are counterstained blue with DAPI. Images were acquired using AxioScan Z1 microscope (Carl Zeiss) at 20× magnification and processed using Zenlift and ImageJ software. (**E**) Knockout of AC5 inhibits kidney enlargement caused by collecting-duct-specific deletion of *Pkd2*. Kidneys were collected from P14 mice with the indicated genotypes (all are Pkhd1/Cre-positive) and weighed. The ratio of kidney weight to body weight is shown. Deletion of *Pkd2* (hatched bar) causes kidney enlargement compared to wild-type mice (filled bar). Concomitant deletion of AC5 in *Pkd2* mutant mice reduces kidney enlargement (stippled bar) and has no effect in wild-type mice (open bar). Error bars represent SEM (n=9–17).

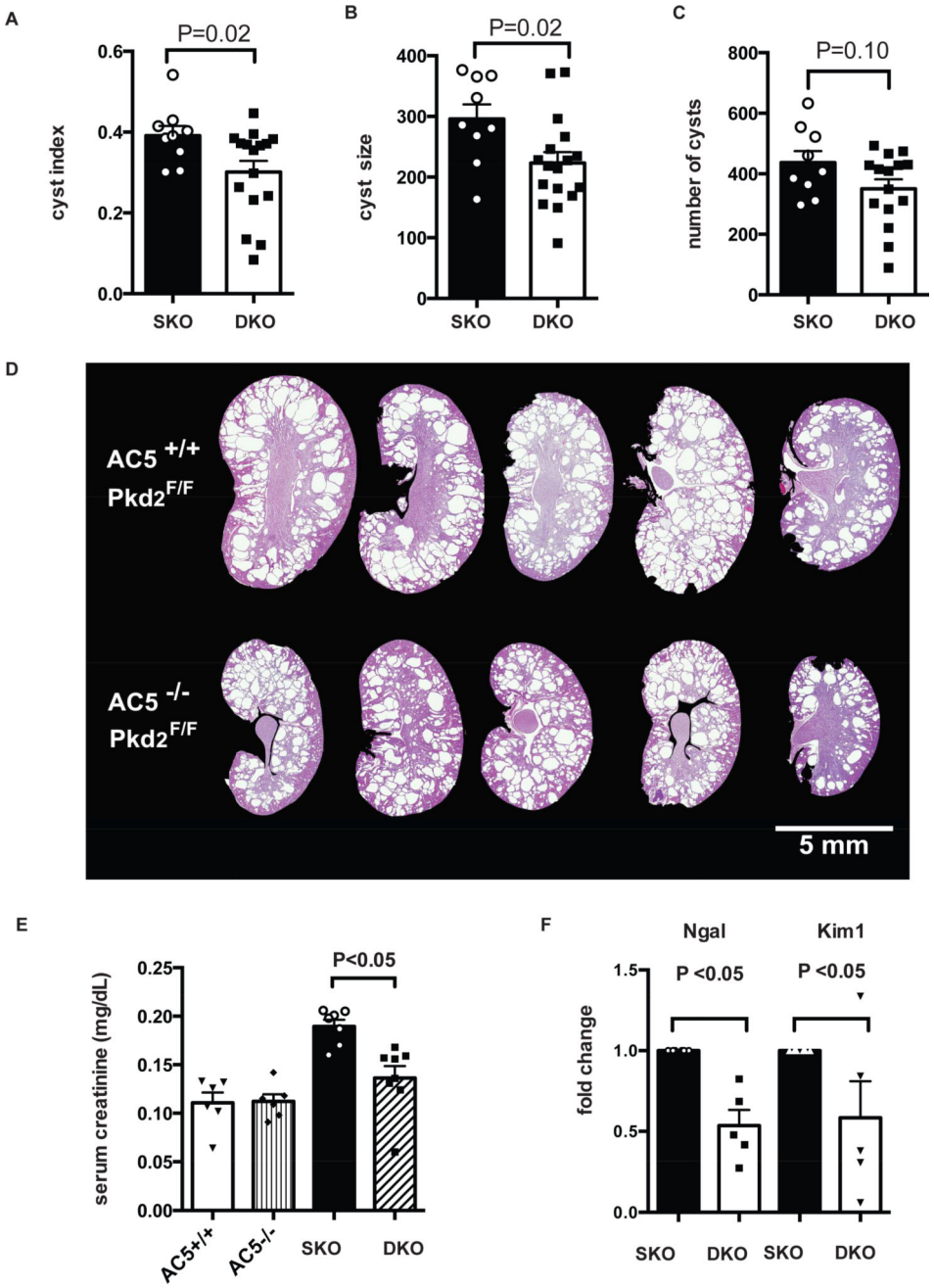

Figure 3. Ablation of AC5 slows cyst progression caused by kidney-specific deletion of *Pkd2*

(**A**) Cyst index of kidneys from *Pkd2*/AC5 double knockout mice (DKO: AC5$^{-/-}$;*Pkd2*$^{F/F}$;Pkhd1/Cre) is lower than *Pkd2* single knockout mice (SKO: AC5$^{+/+}$;*Pkd2*$^{F/F}$;Pkhd1/Cre) at P14. (**B**) Average size of cysts in kidneys from DKO mice is lower than SKO mice at P14. (**C**) Average number of cysts per kidney sagittal section in DKO mice is not significantly different from SKO mice at P14. (**D**) H&E staining of kidneys at P14 shows less severe cystic disease and smaller kidneys in five representative DKO mice (lower panel) compared to SKO mice (upper panel). (**E**) Serum creatinine is elevated in *Pkd2* mutant mice (filled bar) compared to wild-type littermates (open bar) at P14.

Concomitant ablation of AC5 normalizes serum creatinine (hatched bar). Deficiency of AC5 by itself does not affect serum creatinine compared to wild-type mice (vertical bars). Error bars represent SEM (n=7–8). (**F**) qRT-PCR analysis shows that the expression of the kidney injury markers Ngal and Kim-1 is reduced in kidneys from DKO mice compared to SKO mice at P14. Error bars represent SEM (n=4).

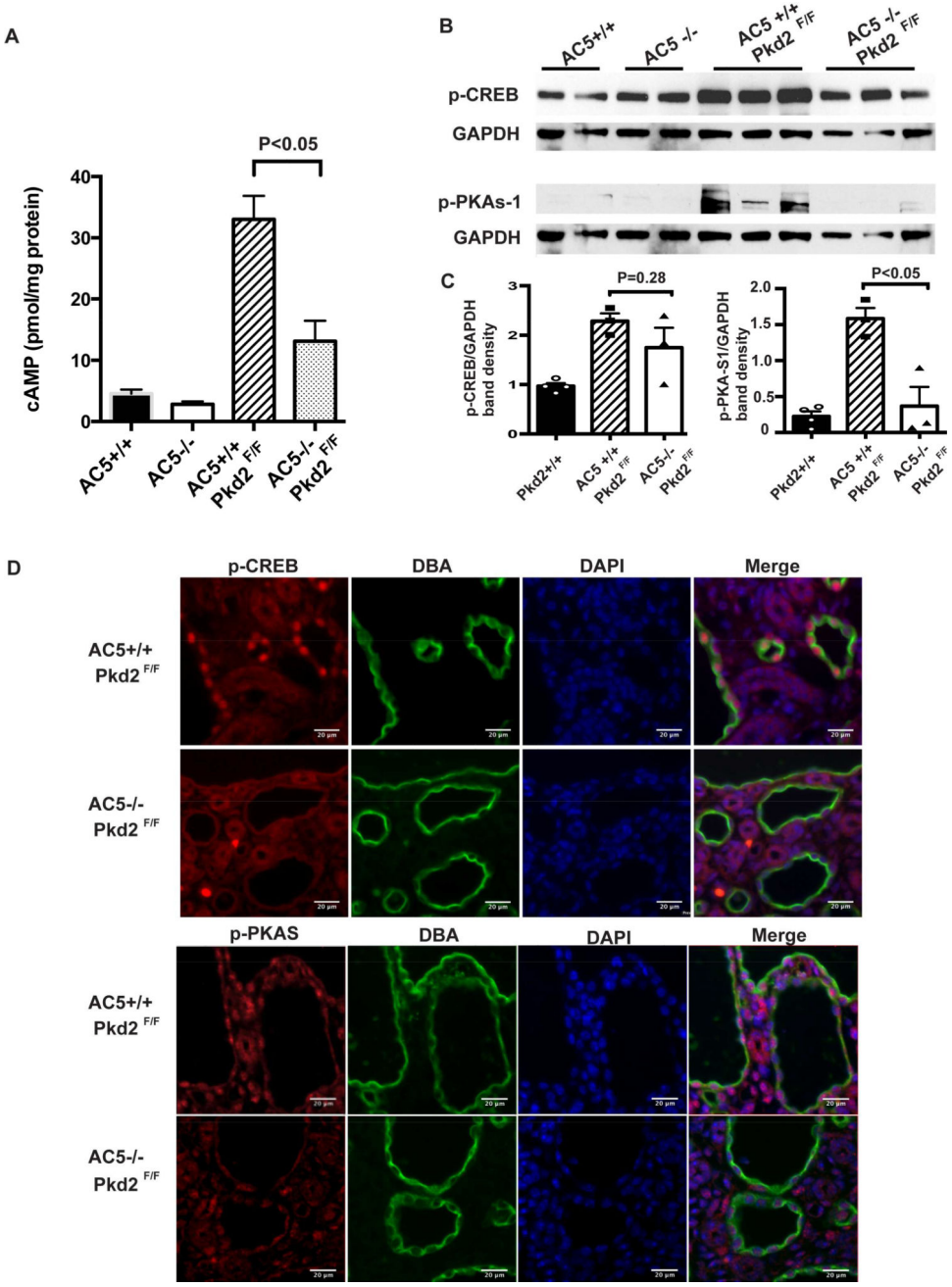

Figure 4. Knockout of AC5 reduces cAMP levels and attenuates cAMP-dependent signaling in *Pkd2* mutant kidneys

(**A**) cAMP levels are significantly elevated in *Pkd2* mutant kidneys at P14 (hatched bar) compared with wild-type kidneys (filled bar). Concomitant ablation of AC5 significantly reduces cAMP levels in *Pkd2* mutant kidneys (stippled bar). (**B**) Immunoblot analysis shows that pCREB and pPKA substrate1 are increased in *Pkd2* mutant kidneys ($AC5^{+/+}$;$Pkd2^{F/F}$) compared to wild-type controls ($AC5^{+/+}$). Concomitant ablation of AC5 reduces CREB phosphorylation (pCREB) and phosphorylated PKA substrates (pPKA-S1) in *Pkd2* mutant kidneys ($AC5^{-/-}$;$Pkd2^{F/F}$). Mice also carried the Pkhd1/Cre transgene. 20 μg protein was used for the analysis, and GAPDH was used as a loading control. (**C**) Quantification by band

densitometry shows that phosphorylated PKA substrates are significantly increased in SKO kidneys (hatched bars) and reduced in DKO kidneys (open bars). pCREB is elevated in SKO kidneys and shows a trend towards reduction in DKO kidneys that was not statistically significant. GAPDH was used for normalization. Error bars represent SEM (n=3). (**D**) Indirect immunofluorescence on kidneys from P14 mice shows reduced nuclear staining of pCREB and pPKA-S1 in collecting ducts of DKO mice ($AC5^{-/-}$;$Pkd2^{F/F}$) compared to SKO mice ($AC5^{+/+}$;$Pkd2^{F/F}$). Red: pCREB (1:400), pPKA-S1 (1:400). Green: FITC-DBA (1:1,000). Blue: DAPI.

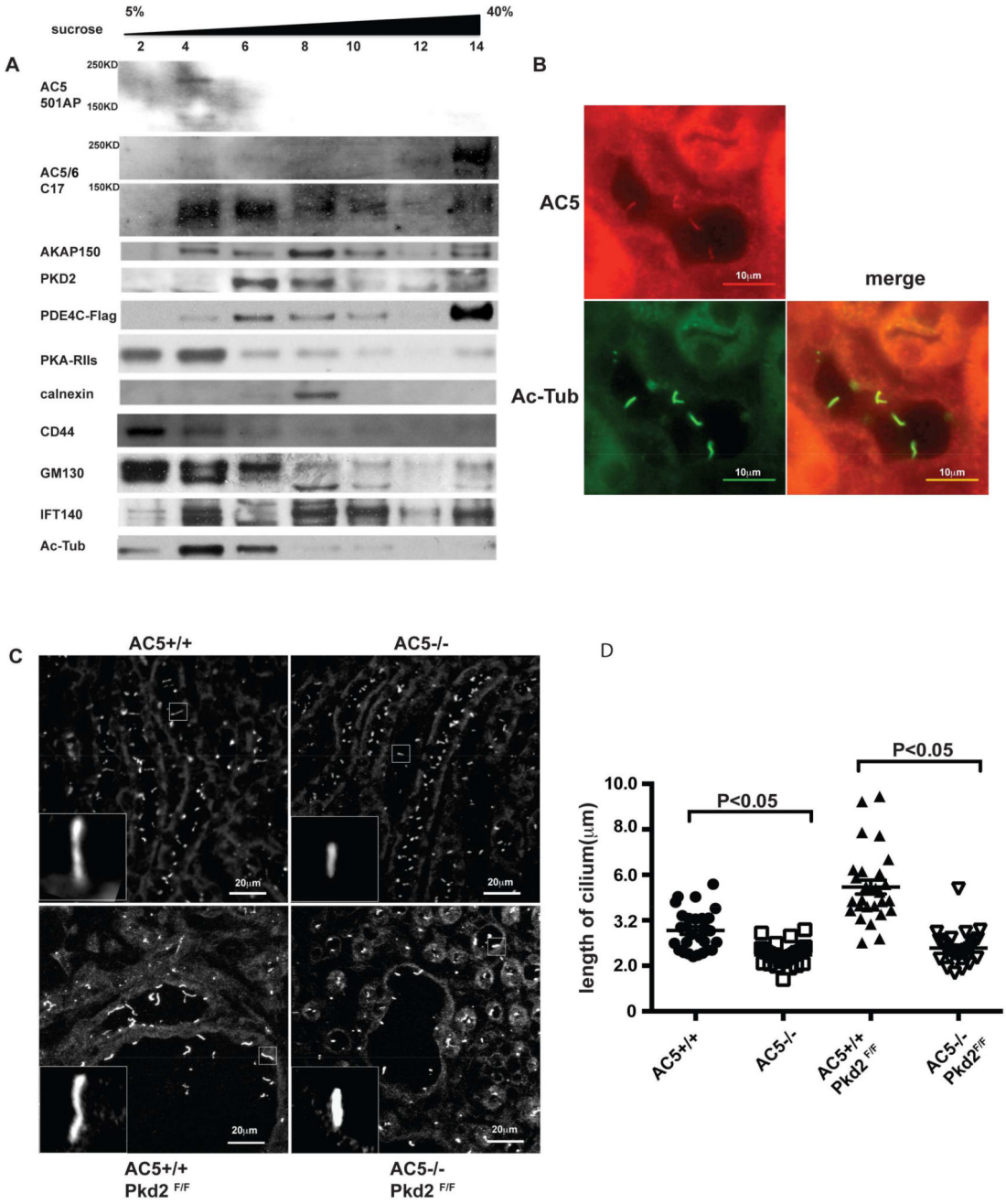

Figure 5. AC5 is located in renal cilia and AC5 deficiency reduces ciliary elongation in *Pkd2* mutant kidneys

(**A**) Sucrose density gradient centrifugation showing co-fractionation of AC5 with ciliary proteins in *Pkd2*$^{2+/-}$ renal epithelial cells transfected with PDE4C-Flag. Fractions were analyzed by SDS-PAGE followed by immunoblotting with antibodies against AC5 (501AP) and markers of Golgi (GM130), endoplasmic reticulum (calnexin), plasma membrane (CD44), and primary cilia (acetylated α-tubulin, Ac- Tub; intraflagellar transport protein 140, IFT140). AC5 is enriched in fraction 4 and to a lesser extent fraction 6, which contain acetylated α-tubulin, IFT140, polycystin-2 (*PKD2*), PDE4C (anti-Flag), AKAP150, and PKA regulatory subunit II (PKA-RII). Immunoblotting with an antibody that recognizes

both AC5 and AC6 (C17) also shows expression in cilia as well as other organelles. (**B**) Indirect immunofluorescence of wild-type mouse kidney sections stained with anti-AC5 antibody (PAC-501AP). Endogenous AC5 is located in the primary cilia of renal tubular epithelial cells in addition to the cell body. Cilia were co-stained with an antibody against acetylated α-tubulin. (**C**) Indirect immunofluorescence showing primary cilia in renal collecting ducts from wild-type mice ($AC5^{+/+}$), AC5 knockout mice ($AC5^{-/-}$), *Pkd2* single knockout mice ($AC5^{+/+}$;$Pkd2^{F/F}$), and *Pkd2*/AC5 double knockout mice ($AC5^{-/-}$;$Pkd2^{F/F}$). Mice were euthanized at P14, and primary cilia were stained with anti-ARL13B antibody (1:400). Insets show that ablation of AC5 reduces ciliary length compared to wild-type and *Pkd2* mutant mice. (**D**) Quantification shows elongation of primary cilia in *Pkd2* mutant mice. Concomitant ablation of AC5 normalizes cilia length. Cilia length was measured using ImageJ after 3D reconstruction of Z-stack images. Statistical analysis was performed with GraphPad Prism 6 using ANOVA for multiple comparisons. Error bars represent SEM.